High resolution spectroscopy with the Reflection Grating Spectrometer onboard XMM-Newton.
An application to the radio galaxy Cygnus A.

E. Torresi

1 Introduction

Since the launch of the two satellites Chandra and XMM-Newton, in 1999, it has been possible to make high resolution spectroscopy in the X–ray band, thanks to the gratings on board them.

XMM-Newton carries two identical gratings that work in the band 6–38 Å(0.3–2 keV). This band contains the K–shell transitions of elements like oxygen, neon, silicon, carbon, nitrogen, magnesium, sulphur and calcium, and the L–shell transitions of heavy elements, in particular the iron L–shell transitions. Moreover the He–like triplets of light elements are contained.

An accurate analysis of these spectral features permits the determination of the physical characteristics of the emitting region like density, temperature, ionization state and elemental abundances.

This kind of study is based on the dependence of the spectral properties of the medium from the excitation processes, collisional or photoionized, and is also based on the state of the medium, transient or quiescent, and on whether the plasma is optically thick or thin.

Through gratings it is possible to disentangle these structures, and recognize the diagnostic tools that permit to trace the origin of the plasma.

Section 2 describes the instrument in its components, and its functioning. In section 3 an example of RGS study is proposed, applied to the case of the radio galaxy Cygnus A.

2 The Reflection Grating Spectrometer (RGS)

XMM-Newton carries six scientific instruments that are co–aligned in the spacecraft, and work simultaneously.

These instruments are:

- **European Photon Imaging Cameras (EPIC)**, three CCDs of two different types, MOS and pn;

- **Reflection Grating Spectrometer (RGS)**, two identical spectrometers dedicated to high resolution spectroscopy;

- **Optical Monitor (OM)**, designed for optical/UV imaging, it works in the 1700–6000 Åband, and is suitable for observation of faint stars ($m_V \leq 7.4$ mag).

The EPIC CCD cameras have moderate spectral resolution ($E/\Delta E \sim 20 - 50$), while the RGS spectrometers have a resolving power $E/\Delta E \sim 150 - 800$ (1st spectral order).
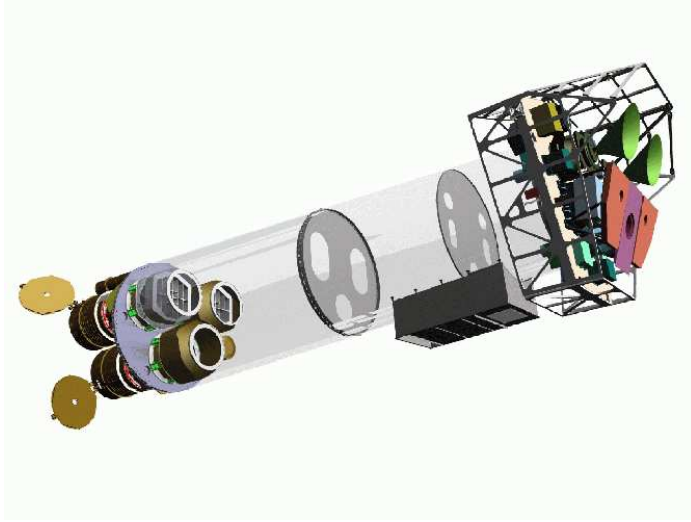
Figure 1: The XMM-Newton payload. At the lower left there are the three mirror modules, two of which are equipped with RGS. At the right end there are the EPIC MOS cameras and their radiators (black/green cones), the EPIC pn camera and its radiator (violet) and those of the RGS detectors (light blue).

Two identical RGS are located behind the two mirror modules associated with the two MOS cameras.

Each RGS is composed by an array of reflection gratings placed in the converging beam at the exit from the telescope.

The functioning of gratings is based on the *diffraction of light*. The light blazes the surface of the grating at an angle α, and emerges at β, following the relation $cos\beta = cos\alpha + m\lambda/d$, where m is the spectral order and d is the groove spacing.

X–rays are reflected at first and second spectral order at the highest efficiency, producing the more interesting data. Counts obtained at the third order are about eight times lower than those at second order, so that statistics becomes poor.

A consequence of the equation of the diffraction of light is that several orders superpose to the CCDs of the RGS focal camera (RFC). An intrinsic energy resolution of the CCD ($\sim$ 160 eV FWHM@2 keV) is required to separate these orders of dispersion.

The RGS in divided in two components:

- *The Reflection Grating Array (RGA)*, contains 182 identical reflection gratings aligned, mounted at grazing incidence in the in–plane and are oriented so that the angle of the incident X–ray at the center of the grating α, is the same for all the gratings in the array.
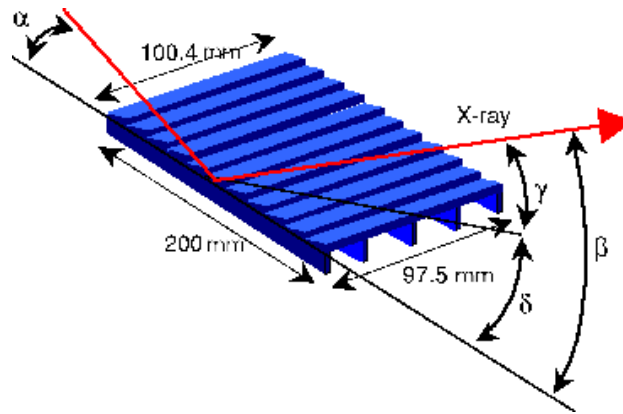
Figure 2: Scheme of a grating with the key dimensions and angles: α is the angle of incidence, β is the diffraction angle for λ_{blaze}, that is the 1st order blaze wavelength. δ is the blaze angle of facets, γ is the graze angle of facets. Each grating measures about 10×20 cm^2.

The separation between the gratings is chosen to be as close as possible. In this way only a part of the beam is intercepted by the RGA, in particular $\eta = sin\alpha / sin\beta_{blaze} = 0.53$, so the 53% of the light is deflected toward the RGA, while the 44% of the undeflected light is intercepted by the MOS cameras in the telescope focal plane. The rest of the light is absorbed by the RGA itself.

These gratings needs to be very flat in the long direction in order to avoid a degradation of the resolution. The grating substrates consist of 1 mm SiC face sheets.

- *RGS Focal Camera (RFC)*, is constituted by three thermal nested shells: a CCD bench and two heatshields. The CCD bench contains 9 CCDs back–illuminated, in order to maximize the response of the instrument in the soft band. This side of the CCD bench interfaces to a coldfinger which provides the necessary cooling and ensures a uniform temperature of about –80°.
  The opposite side of the CCD bench is recovered of a heatshield of thin aluminium, whose role is to suppress the optical/UV radiation inevitably reaching the detector.
  Each CCD has 1024×768 pixels ($27 \times 27 \ \mu$m^2): one half of the CCD is

4

exposed, while the other half is used a storage area.

After the first week of operation a problem occured to the CCD ♯4 in RGS2, and affected the wavelenght range 20.1–23.9 Å. A similar fate affected CCD ♯7 of RGS1 several months later, in the 10.5–14 Åband.

For this reason the operational conditions of the instrument have been modified to reduce the load of the two CCDs to a minimum.
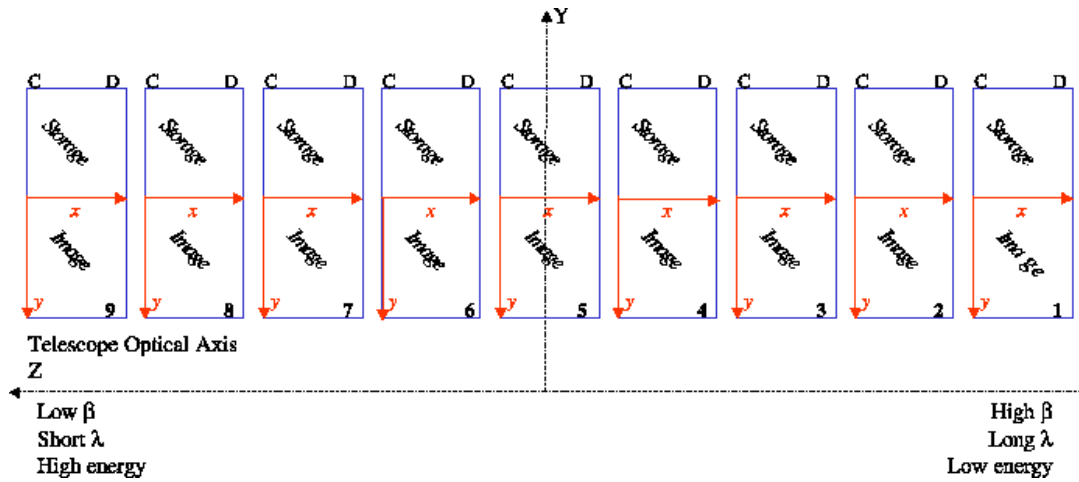

Figure 3: Representation of the 9 CCDs composing the RFC. One half of each CCD is exposed to X–rays, the other half is left as a storage area. The dispersion direction is along the Z axis, in this way higher energies are dispersed to higher value in Z.

The detector is operated in frame transfer mode, in order to obtain optimum scientific performance. In this way the image is accumulated in one half of the CCD ("image" section) and then is quickly (20 msec) transferred to the other half ("storage" section). Here it is read out through two low noise serial output registers.

This rapid transfer prevent the data from smearing during the read out phase.

The RGS has three operating modes:

1. SPECTROSCOPY: is the most common mode used in flight. Each

CCD is read out one after the other, in frame transfer mode, with a grouping of 3×3 on chip. The minimum accumulation time is therefore 5.7 seconds.

2. HIGH TIME RESOLUTION: this mode allows to reach the shortest accumulation time (15 msec) if only one CCD is read out.

3. DIAGNOSTIC: the full image is directly transferred from the CCD to the ground, so the on–board processing is completely bypassed. These data are transferred very quickly to the ground, less than 1 minute at a speed of 22 kbit/sec, and are used for dark current and system noise level verification.

The in–flight performance of the RGS is estimated through the following parameters:

- LINE SPREAD FUNCTION (LSF) is a convolution of the mirror response and the grating response, followed by the convolution with the detector response. It depends on the proper alignment of these components.
In addition there is a significant component due to scattering on the surfaces of the mirrors and the gratings, and is most significant at the shortest wavelenghts and the highest diffraction orders.

- RESOLVING POWER is the ability to detect weak emission lines above the background or the continuum. It is better measured by the half energy width (HEW) of the profile, that is more dependent on the amplitude and widths of the scattering wings at short wavelenghts.
Despite the differences of manifactures of the two RGS are few, their energy resolutions differ because of the different focussing. However their resolving power agree with expected value that is ∼800 HEW at the longest wavelenghts.

- SPECTRAL RESOLUTION it depends on the angular extension of the observed object. For extended sources the emission lines are broadened following the relation $\Delta\lambda(ext) = 138\ \theta(ext)/m$, where $\Delta\lambda(ext)$ is the resolution in Å, and $\theta(ext)$ is the source extension in arcmin.
For point sources the RGS work better than the EPIC camera.

- EFFECTIVE AREA the parameters involved in the determination of this quantity are: the properties of all the optical components located along the light path, the quantum efficiency of the CCDs, the geometry and efficiency of the grating, and vignetting factors.

The measurement of wavelengths with RGS is accurate to 8 mÅ across the entire wavelength band, this result is based on the distribution of wavelength residuals of the calibration lines.
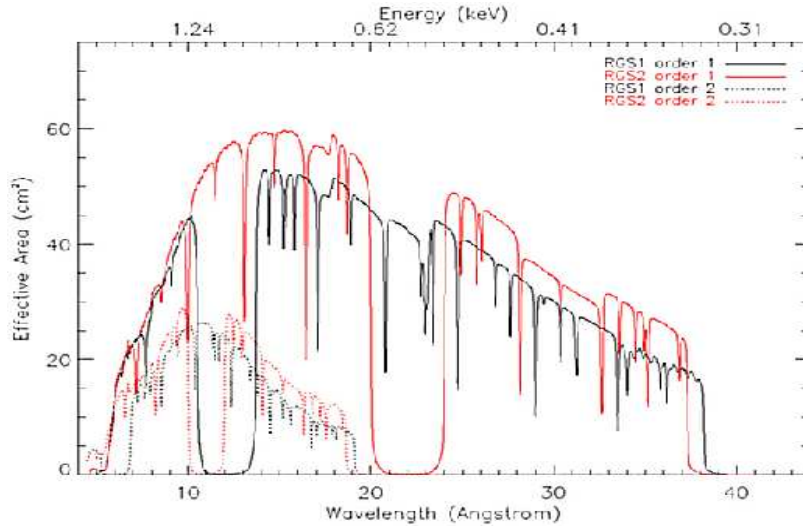

Figure 4: Effective area of both RGS as a function of energy and wavelenght.

In Tab.1 are summarized the key performance parameters:

Table 1: Key parameters

PARAMETER	VALUE	COMMENT
A_{eff}	140 cm^2	peak effective area
λ	6-38 Å	wavelenght range first order
$\lambda/\Delta\lambda(FWHM)$	100-500	resolution (line separation)
$\lambda/\Delta\lambda(HEW)$	100-800	resolution (weak line detection)
$\delta\lambda$	8 mÅ	wavelenght accuracy

3 An application: the RGS study of the radio galaxy Cygnus A

Cygnus A (3C405) is one of the brightest radio galaxy of the 3C catalogue. It is very nearby (z=0.056), and is immersed in a rich cluster, which makes hard the study of its X–ray spectrum.

It is a Fanaroff–Riley type II (FRII) radio galaxy, classified as a Narrow Line Radio Galaxy (NLRG) because of its optical spectrum.

As all the AGN radio–loud its hard X–ray spectrum is well represented by a heavily absorbed power law ($N_H \sim 2.1 \times 10^{23}$ cm^{-2}), where the same absorbing cold gas probably produces the Fe Kα line at 6.4 keV.

The origin of the soft emission in the 0.5–2 keV band is still debated. In Seyfert 2 galaxies, considered the analogous radio–quiet of NLRGs in the unification model, the soft emission has been interpreted as emission from photoionized gas, thanks to the gratings on board XMM–Newton and Chandra, that can disentangle the emission lines.

For NLRGs the current hypothesis is that the soft emission is due to the jet originating in the outer edge of the torus [Hardcastle & Worral, 1999; Belsole et al, 2006].

Cygnus A shows a nucleus similar to the ones of Sy 2 galaxies, with a central component coincident with the radio core of hard X–ray emission (E>2 keV), and two regions of softer emission (E<2 keV), located at 1.2″ NW and SE from the center.
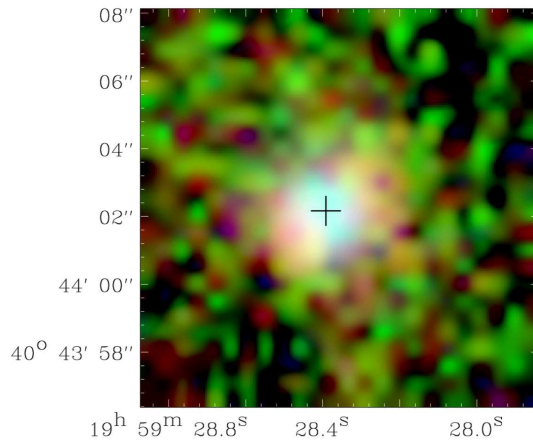

Figure 5: Color representation of the *Chandra* X–ray image of the nucleus of Cygnus A.

The pn spectrum shows an excess of emission around 1 keV, that can be interpreted as a blend of emission lines which the moderate resolution of the pn can not disentangle.
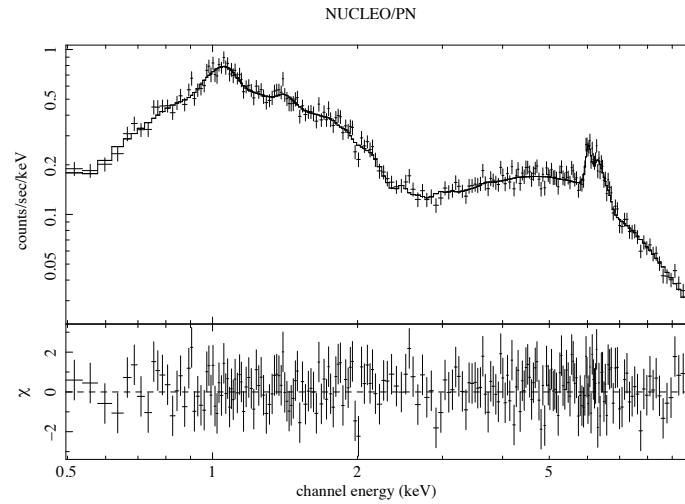

Figure 6: X–ray spectrum of the nucleus of Cygnus A extracted from the pn data. The *upper* panel shows the data points with error bars (crosses), with the model folded through the instrument responses (solid lines passing through the data points). The *lower* panel shows the χ residuals from the fit.
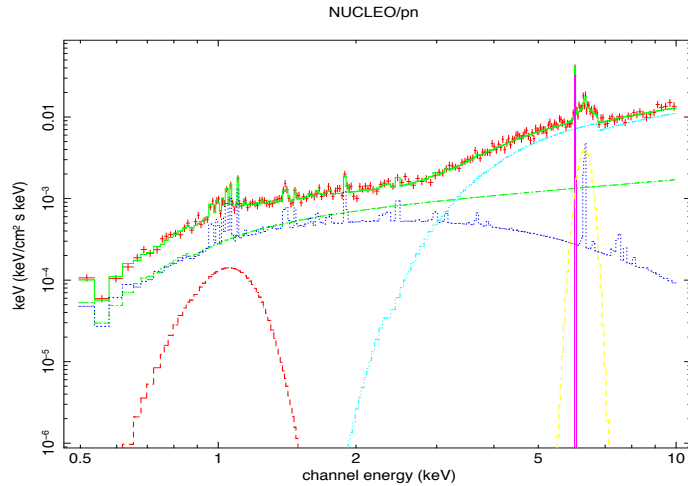
Figure 7: Spectral model used to fit the data of the nucleus of Cygnus A.

For this purpose the RGS data have been analyzed. Thanks to its unprecedented sensitivity and energy resolution, the RGS can distinguish fine structures. As mentioned in the introduction there are two types of plasma that can produce X–ray emission lines:

- collisionally ionized plasma

- photoionized plasma

There are some diagnostics that permits to distinguish between them, like the radiative recombination continua (RRC), or the He–like triplets of oxygen and neon.

DATA ANALYSIS

The analysis of the RGS data is structured in several phases.

1st step: the RGS data were taken simultaneously to those of the three EPIC camera. The duration of the observation is 22.5 ksec.

The RGS worked in normal spectroscopy mode. The XMM environment has been set with SAS version 6.5.

In order to create the event files relative to the two RGS instruments, the command **rgsproc** has been launched. This command creates the event files starting from the ODF.

2nd step: once all the files are available, the next step is to verify the accuracy of the coordinates used for the prime source. The accuracy of the *rgsproc* depends critically from this parameter.

The command *fv* followed by the source list, permits to visualize two sets of coordinates: PROPOSAL, which gets the position from the target coordinates as given in the proposal, and is the prime source, and ON AXIS. This latter set of coordinates is calculated from the spacecraft attitude.

The coordinates of Cygnus A were correct, so it was not necessary an additive

adjustment.

3rd step: before starting the analysis there were displayed the dispersion vs cross dispersion and dispersion vs energy images, and overlayed the selected region masks (Fig.8). With the task *evselect* it is possible to select the event file and determine the image name. In this phase two corrections are introduced, one for each axis: the BETA_CORR and the XDSP_CORR. β is the dispersion angle, while XDSP is the cross dispersion angle, and together they define the dispersion coordinates, based on the position and orientation of the RGA.
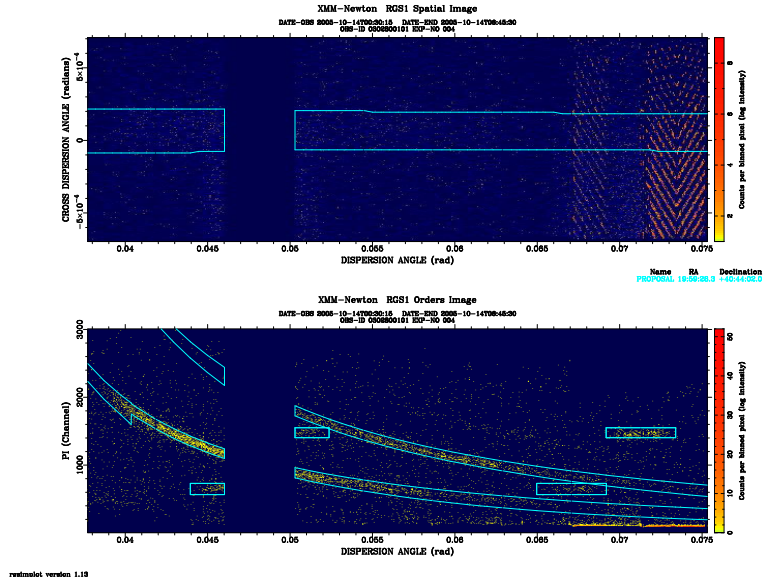

Figure 8: The *upper* panel represents the spatial dispersion of radiation from Cygnus A in RGS1. The *lower* panel shows the dispersion of radiation at first and second order.

The RGS instruments dispers the light only in one direction, so it is not possible to select a particular region where extract the spectrum to analyze. The command *xpsfincl* allows to reduce or extend the mask along the cross dispersion angle (y axis). By default the selection mask corresponds to a region equal to 90 % of the PSF.

In the case of point like sources it is not a problem, but in Cygnus A this could constitute a hindrance because of the presence of the cluster. So it was decided

11

to reduce the mask at the 67 % of the PSF.

4th *step*: while in the analysis of the EPIC data you need to extract a light curve and create a Good Time Intervals file (GTI), in the RGS the creation of GTI is optional. Infact RGS event lists have one GTI extension for each chip generated by rgsproc, these GTI define good periods based on the attitude and housekeeping data included on the ODF.

The task *rgsproc* creates also the response matrix **rgsrmfgen**.

5th *step*: in most cases celestial sources are weak for RGS, which produces low signal–to–noise spectra. So it is important to use the correct statistics in order to keep the high energy resolution typical of the instrument. The χ^2 statistics does not apply to spectra limited by low number of counts, so the spectra were rebinned using the task rgsproc rebin=5, and during the analysis the C–statistics has been adopted.

RESULTS

Finally the two RGS spectra were summed, and it was analyzed the total spectrum. This spectrum showed a continuum that was fitted with a *mekal* model in order to reproduce the thermal emission of the cluster.

Then a gaussian in the model was added for each energy excess in the spectrum, calculating the centroid energy and the corresponding wavelength.

Successively those parameters were compared with the literature, in particular with the CHIANTI Atomic Database [Dere et al., 2001] and the work of Kinkhabwala on the photoionized gas in NGC 1068.

Most of the emission lines are found to be produced by thermal, collisional gas, for example FeXXIV, SiXIV, OVIIILyβ, NeXLyα.

Nevertheless other lines like the resonance lines of OVII and NeIX are produced by collisional gas only invoking a temperature less than 1.5 keV, never observed for the cluster surrounding Cygnus A.

Maybe those lines are hints of photoionized gas [Kinkhabwala et al., 2002; Guainazzi & Bianchi, 2007], even if for the forbidden lines it is only could possible to determine an upper limit in the intensity, because of the low statistics. The ratios between the intensity of resonance and forbidden lines are in agreement with these of a photoionized gas.

Fig.9 represents the RGS spectrum divided in three energy bands: 0.5–1 keV, 1–1.5 keV, 1.5–2 keV.
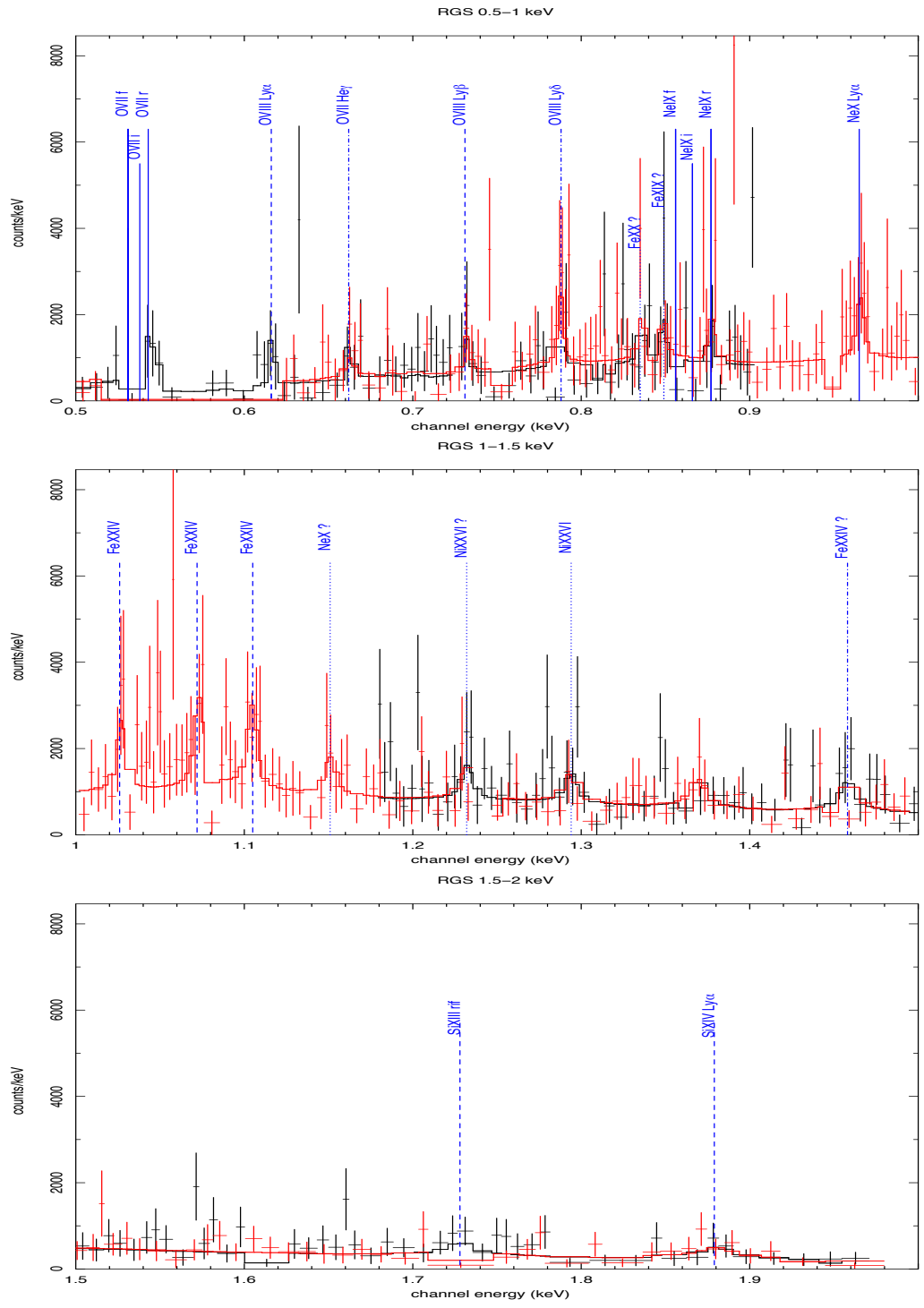
Figure 9: First order RGS spectra (RGS1 + RGS2) of Cygnus A. *Upper* panel: 0.5–1 keV; *medium* panel: 1–1.5 keV; *low* panel:1.5–2 keV. Each line is identified with the final stage of the ion. *Solid lines*=lines that could be associated with photoionized gas. *Dashed lines*=lines emitted by the cluster. *Dotted lines*=lines with unclear origin.

13

Table 2: Righe osservate nello spettro dell'RGS con possibile identificazione, relativa lunghezza d'onda teorica e osservata, energia osservata, intensità, e tipo di plasma.

Possibile ID[a]	λ_T [Å]	λ_O^b [Å]	E^c [keV]	Intensità	Plasma
OVII(r)	21.602	$22.833^{+0.167}_{-0.042}$	$0.543^{+0.004}_{-0.001}$	$2.6^{+3.07}_{-2.28} \times 10^{-4}$	Fotoionizzato?
OVII(i)	21.803	23.04	0.538^d	$< 1.57 \times 10^{-4}$	Fotoionizzato?
OVII(f)	22.101	23.34	0.531^d	$< 4.27 \times 10^{-4}$	Fotoionizzato?
NeIX(r)	13.447	$14.13^{+0.03}_{-0.1}$	$0.877^{+0.002}_{-0.006}$	$2.67 \pm 2.5 \times 10^{-5}$	Fotoionizzato?
NeIX(i)	13.552	14.31	0.866^d	$< 0.571 \times 10^5$	Fotoionizzato?
NeIX(f)	13.698	14.41	0.86^d	$< 3.2 \times 10^{-5}$	Fotoionizzato?
NeX Lyα	12.134	$12.84^{+0.04}_{-0.12}$	$0.965^{+0.0032}_{-0.0057}$	$3.24^{+3.27}_{-2.29} \times 10^{-5}$	Collisionale
OVIII Lyδ	14.89	$15.73^{+0.07}_{-0.04}$	$0.788^{+0.0037}_{-0.0020}$	$3.71^{+4.4}_{-2.5} \times 10^{-5}$	Collisionale?
OVIII Lyβ	16.006	$16.96^{+0.05}_{-0.04}$	0.731 ± 0.02	$2.5^{+3.19}_{-2.22} \times 10^{-5}$	Collisionale
OVIII Lyα	18.969	$20.12^{+0.1}_{-0.33}$	$0.616^{+0.003}_{-0.01}$	$7.56^{+8.8}_{-7.4} \times 10^{-5}$	Collisionale
OVII Heγ	17.768	$18.72^{+0.04}_{-0.06}$	$0.662^{+0.0017}_{-0.0021}$	$3.96^{+5.24}_{-3.14} \times 10^{-5}$	Collisionale?
SiXIV Lyα	6.18223	$6.598^{+0.042}_{-0.049}$	$1.879^{+0.012}_{-0.014}$	$6.4^{+1.96}_{-3.93} \times 10^{-5}$	Collisionale
SiXIII (rif)	6.79	$7.17^{+0.04}_{-0.001}$	$1.728^{+0.009}_{-0.014}$	$< 4.51 \times 10^{-5}$	Collisionale
FeXXIV	10.62	$11.22^{+0.04}_{-0.03}$	1.105 ± 0.003	$5.16^{+3.78}_{-2.68} \times 10^{-5}$	Collisionale
	11.03	$11.56^{+0.03}_{-0.05}$	$1.072^{+0.003}_{-0.005}$	$5.12^{+3.26}_{-3.01} \times 10^{-5}$	Collisionale
	11.43	$12.08^{+0.02}_{-0.09}$	$1.026^{+0.002}_{-0.008}$	$3.76^{+2.6}_{-3.0} \times 10^5$	Collisionale

(a) CHIANTI ATOMIC DATABASE [Dere et al., 2001]
(b) $\lambda_O = \lambda_T * (1 + z)$
(c) E(keV)$= \frac{12.3985}{\lambda(\mathring{A})}$
(d) Valore fissato all'energia aspettata.

4   Conclusions

The nature of the soft emission in NLRGs is not clear yet. At the moment the favourite hypothesis predicts that this emission is due to the jet leaving the outer edge of the torus.
Nevertheless another hypothesis can not be ruled out: emission from photoionized gas, according to the soft emission of Seyfert 2 galaxies.
The soft X–ray band study of the radio galaxy Cygnus A with the RGS described in this report indicates hints of photoionized gas.
The high spectral resolution of the RGS can be used to study a standard sample of radio galaxies, and to throw light on the problem of the origin of the soft emission.

5   References

XMM–Newton User's Handbook *http://xmm.vilspa.esa.es/external/xmm_user_support /documentation/uhb_frame.shtml.*

Belsole E., Worral D.M., Hardcastle M.J., 2006, MNRAS, 366, 339.

den HerderJ.W., Brinkmann A.C., Kahn S.M., Branduardi–Raymont G., et al., 2001, A&A, 365, 7.

Dere K.P., Landi E., Young P.R., Del Zanna G., 2001, ApJS, 134, 331.

Hardcastle M.J., Worrall D.M., 1999, MNRAS, 309, 969H.

Kinkhabwala A., Sako M., Behar E., Kahn S.M., Paerels F., Brinkmann A.C., Kaastra J.S., Gu M.F., Liedhal D.A., 2002, ApJ, 575, 732.

Kinkhabwala A., 2003, PhD Thesis.

APPENDIX A

Here the principal commands used in the RGS analysis are described [1].
After setting the XMM environment with the current version of the SAS, the next command to launch is:

- **rgsproc**, it creates the event files relative to the two RGS instruments, starting from the "raw" ODF data. This process may take 5-10 minutes depending on the ODF size.
  Now in the working directory there are the following files:

    - PxxxxxxyyyyR1eeeEVENLI0000.FIT [2]: the event list;
    - PxxxxxxyyyyR1eeeeSRSPEC1001.FIT: spectrum of the source and relative background (1° order);
    - PxxxxxxyyyyR1eeeeBGSPEC1001.FIT: background spectrum (1° order);
    - PxxxxxxyyyyR1eeeeSRSPEC2001.FIT: spectrum of the source and relative background (2° order);
    - PxxxxxxyyyyR1eeeeBGSPEC2001.FIT: background spectrum (2° order);
    - PxxxxxxyyyyR1eeeeSRCLI_0000.FIT: source list;
    - PxxxxxxyyyyR1eeeeRSPMAT1000.FIT: response matrix (1° order);
    - PxxxxxxyyyyR1eeeeRSPMAT2000.FIT: response matrix (2° order);
    - PxxxxxxyyyyR1eeeeOBX000fluxed1000.FIT: combined fluxed 1° order spectrum;
    - PxxxxxxyyyyR1eeeeOBXfluxed2000.FIT: combined fluxed 2° order spectrum.

  The last two files can be used to have a qualitative idea of the data trend, but cannot be used for a quantitative analysis.
  All the files above are created during five stages of reprocessing:

    1. EVENTS: it comprises preliminary tasks and source-indipendent calibrations. During this stage the attitude-drift GTI, the housekeeping GTI and the source list are created. This is why it is not necessary to construct a further GTI file;

    2. ANGLES: in this stage the event coordinates are corrected for aspect drift, where corrections are specific to the chosen primary source. Also the dispersion and cross-dispersion channels are defined, according to which the events and exposure are binned;

---

[1] For more informations: **http://xmm.esac.esa.int/sas/7.1.0/documentation/threads/rgs_thread.html**
[2] xxxxxx indicates the proposal number, yyyy is the observation, R1 refers to the instrument e.g. RGS1, and eeee is the RGS exposure identifier.

3. FILTER: this stage filters the combined event list to produce the filtered event list. The main aim is to remove data that are not useful for the analysis;

4. SPECTRA: it creates spectra at each specified reflection order;

5. FLUXING: it creates the fluxed spectrum of the primary source, and the response matrix.

The default stages of entrance and output are ♯1 e ♯5, otherwise it is possible to select a particular stage ("*entrystage*") without restart the entire process.

- **fv PxxxxxxyyyyR1eeeeSRCLI_0000.FIT**, with this task it is possible to verify the accuracy of the coordinates used for the prime source, from which the accuracy of the *rgsproc* depends. Selecting the button "*all*" corresponding to the SRCLIST, it permits to visualize two sets of coordinates, as showed in Fig. 10. It is important that the PROPOSAL coordinates agree with the source coordinates.

Figure 10: Sets of coordinates. The "PROPOSAL" coordinates get the position from the target coordinates given in the proposal, while the "ONAXIS" coordinates are calculated from the spacecraft attitude.

- **evselect table='PxxxxxxyyyyR1eeeeEVENLI0000.FIT:EVENTS' imageset='my spatial.fit' xcolumn='BETA CORR' ycolumn='XDSP CORR'**

  evselect table='PxxxxxxyyyyR1eeeeEVENLI0000.FIT:EVENTS' imageset='my pi.fit' xcolumn='BETA CORR' ycolumn='PI' yimagemin=0 yimagemax=3000 expression='REGION(PxxxxxxyyyyR1eeeeSRCLI 0000.FIT:RGS1 SRC1 SPATIAL, BETA CORR,XDSP CORR)'

  rgsimplot endispset='my pi.fit' spatialset='my spatial.fit' srcidlist='1' srclistset='PxxxxxxyyyyR1eeeeSRCLI 0000.FIT' device=/xs

  With this series of commands it is possible to display the dispersion vs. cross-dispersion and dispersion vs energy images as showed in Fig. 8.
  The RGS instruments are thought to analyze point-like sources, so they dispers the light only in one direction. This could be a problem when an extended source is analyzed, as in the case of Cygnus A, where the radio galaxy is sorrounded by a rich cluster.
  One possible way to solve this problem and minimize the contribution of the cluster, is to reduce the PSF:

- **rgsproc entrystage=4:spectra xpsfincl 67**

  The default value of the PSF is 90%, corresponding to an extraction region of radius $50''$, while the 67% of the PSF corresponds to an extraction region of $15''$ (based on the values of the fractional encircled energy for MOS cameras).
  At this point of data reduction it is possible to create a lightcurve of the pure background events, but this is necessary only in case of high flares. Infact the task *rgsproc* creates a GTI extension for each chip, based on the attitude and housekeeping data included on the ODF.

- **evselect table=PxxxxxxyyyyR1eeeeEVENLI0000.FIT timebinsize=100 rateset=my rgs1 background lc.fit makeratecolumn=yes maketimecolumn=yes expression='(CCDNR==9) &&(REGION(PxxxxxxyyyyR1eeeeSRCLI 0000.FIT: RGS1 BACKGROUND,BETA CORR,XDSP CORR))'**

18

dsplot table=my_rgs1_background_lc.fit x=TIME y=RATE

When flares are visible and have much larger count rates than the average, it may be wise to create a GTI table to be used in conjunction with the internal GTI tables:

- **tabgtigen table=my_rgs1_background_lc.fit gtiset=my_low_back.fit expression='(RATE<r)'**

"r" indicates counts/sec. Its typical values vary in the range 0.1-2 counts/sec.

The response matrix has been created in the 5th stage (fluxing) by the command **rgsrmfgen**.

Celestial sources are typically weak for RGS, so it is useful to rebin the spectrum:

- **rgsproc rebin=5**

where 5 is the minimum number of counts for each channel.

Now the analysis of the RGS spectrum with XSPEC can start.